Mortality in Germany during the Covid-19 pandemic:
discussion paper

Alois Pichler*† Dana Uhlig*

July 28, 2021

Abstract

The Covid-19 pandemic still causes severe impacts to the society and the economy. This paper studies excess mortality during the pandemic years 2020 and 2021 in Germany empirically with a special focus for the life insurer's perspective. Our conclusions are based on official counts of German governmental offices on the living and deaths of the entire population. Conclusions, relevant for actuaries and for specific insurance business lines, including portfolios of pension, life and health insurance contracts, are provided.

Keywords: Excess mortality · parametric models · decreasing mortality rates
Classification: 97M30, 91B30, 62C12, 62F15

1 Introduction

The Covid-19 pandemic hits mortality along all ages. But other factors, in particular governmental measurements during the crises impact the mortality of the population equally well. This study employs parametric mortality models to assess the overall impact of the current situation on mortality and its results should be of interest for life and pension insures and particularly for actuaries managing these portfolios.

Compared to other populations, the German population is specific and unique for historical and political reasons. The mortality rates in former German Democratic Republic (GDR) and the federal republic of Germany (FRG), until its reunification in 1990, are supposedly different. Nowadays, this gap is believed to narrow. This circumstance becomes insignificant for the mortality during the Covid-19 pandemic by reducing ourselves to reliable data after the fall of the iron curtain. Although based on German data with its own limitations and peculiarities, the conclusions of our findings for other European societies with comparable governmental measurements during the crisis are similar.

*University of Technology, Chemnitz, Faculty of Mathematics. 90126 Chemnitz, Germany
†DFG, German Research Foundation – Project-ID 416228727 – SFB 1410. Contact: alois.pichler@math.tu-chemnitz.de

There is evidence, however, that this is not correct for the United States, for example, and other states, which reacted differently during the crisis. We believe that the aspects presented here are of interest for social welfare, social insurance and for private insurers.

For reason already indicated above partially, complete observations of lifespans are not accessible, in general. Migration is one out of many additional components, which impact the mixture or composition of the population and thus the observations available. In periods accessible to observations, individuals either survive or die. From statistical perspective, these partial or limited observations constitute *censored data*.

A further difficulty in investigating mortality related to Covid-19 is that it is the boundary of the observations here, which is of particular interest. That is, it is unavoidable and crucial to focus on the *elder* segment of the entire population. For natural reasons, this fraction of the population scales down rapidly with increasing ages and is the smallest faction overall. Further, the mortality of this particular group behaves presumably different from the larger part of the population in midlife. Precise and ambitious estimates for small population sizes are more challenging here and parametric models can be of help.

Several mathematical models have been developed in the academic literature to capture the peculiarities and specific features of mortality rates, which vary with age, sex, with the progress in medicine in the whole society, perhaps with regions and so on. In general, we distinguish between parametric and non-parametric models and this distinction is of importance here: for a careful investigation of expected deaths in a given period it is essential to achieve high precision, particularly for high ages. But the problem is that this segment of the population is small, for extraordinary high ages even too small. An important justification of the parametric model is the limited data available in general and the desired model precision, addressed in detail further below. References to the literature below provide sufficient evidence and justifications of the parametric approach chosen here.

An analytic mortality model, derived from biological components, apparently, is not at the actuary's disposal yet; but surprisingly, parametric models enjoy a high prediction precision still today. Cairns et al. (2008); Cairns (2000), for example, review elementary building blocks (even in different segments of the insurance business) and relate them to all types of longevity risk and even stochastic mortality. Building on the Lee-Carter model, Czado et al. (2005) investigate parametric mortality projections involving prior distributions in a typical Bayesian approach. Osmond (1985) is an early paper to address the important aspect of mortality rates of cohorts and our modelling shall follow this proposal to some extent. Wong-Fupuy and Haberman (2004) intend to predict, by employing a switching regime approach, mortality trends over years. In contrast, Currie et al. (2004) smooth mortality trends for data dating back half a century, and we pick some suggestions from these learnings. The recent paper Missov et al. (2015) investigates the Gompertz force of mortality in terms of the modal age at death; this gives additional interpretations of the models and the results achieved, which this paper extends. But beyond that, we have found that proper scales, as this paper explains, can help a lot in implementing the procedures adequately. We finally want to mention that

there exist non-parametric approaches as well (see Pichler (1997)), but they are more adequate for the midlife, but less qualified for our purposes with focus on the segment of the elder population; for narrow population sizes they tend to overfitting and to lose prediction power.

Cohen et al. (2018) investigate, if the basic model (cf. Gerber (1997)) is still accurate. They extend even the basic model to better model infant mortality. Brouhns et al. (2002) focus on estimation procedures as (weighted) ordinary least squares and combine further the Lee Carter with Poisson distributions to estimate parameters. The accuracy of these models is investigated for a Belgian cohort. Gavrilov and Gavrilova (2011), finally, investigates mortality rates of advanced ages. Their conclusion on the hazard rate of old ages is important for the approach chosen here, as they do not give significant evidence of an accelerated death model.

We want to finally mention Cairns et al. (2009), who study the mortality of England and Wales, as well as the United States in different parametric models. They discuss eight different parametric models and investigate their accuracy for varying purposes. Cairns et al. (2020) is an early study of mortality during Covid-19 pandemic, with a focus and data from England and Wales, and an intention comparable to this discussion paper.

The human mortality database provides access to observed deaths for different populations, mainly of Western countries;[1] this webpage provides an impressive visualization tool as well[2] cf. Németh et al. (2021) or in *Our World in Data*.[3] As detailed on the data below, some of our computations build on these valuable data sources.

Our approach follows basic ideas elaborated in the long period of preceding investigations. To be most precise on older ages we employ a parametric model; the model is chosen rather simple to avoid over-parametrization and model specific dependencies. What we do take into account, however, is the constant improvement of mortality over time, which was empirically observed during the last decades. To stabilize the statistical results of the estimators we employ maximum likelihood estimation techniques.

Outline. The following Section 2 establishes the mathematical model. Section 3 addresses the estimation procedure and related considerations to assess mortality. Section 5 presents the results for the German population on Covid-19, before Section 6 concludes.

2 The parametric mortality model

The force of mortality (also known as hazard function in reliability theory) corresponding to an $\mathbb{R}_{\geq 0}$-valued random variable with cumulative, differentiable distribution function F is

$$\mu(x) \coloneqq \frac{F'(x)}{1-F(x)} = -\frac{\mathrm{d}}{\mathrm{d}x} \ln\left(1-F(x)\right).$$

[1] https://mortality.org/

[2] https://mpidr.shinyapps.io/stmortality/

[3] https://ourworldindata.org/grapher/excess-mortality-raw-death-count

Employing an antiderivative with[4]

$$M'(x) = \mu(x) \quad (\text{i.e., } M(x) = \int_{x_0}^{x} \mu(s)\,\mathrm{d}s),$$

the corresponding survival function is

$$1 - F(x) = e^{M(0)-M(x)}$$

and the density

$$F'(x) = \mu(x) \cdot e^{M(0)-M(x)}. \tag{2.1}$$

For distributions describing lifetimes it is common practice to set

$${}_up_x \coloneqq \frac{1-F(x+u)}{1-F(x)} = e^{-\int_x^{x+u}\mu(s)\,\mathrm{d}s} = \exp\big(M(x) - M(x+u)\big) \tag{2.2}$$

and

$${}_uq_x \coloneqq 1 - e^{-\int_x^{x+u}\mu(s)\,\mathrm{d}s} = 1 - \exp\big(M(x) - M(x+u)\big) \tag{2.3}$$

for the probability of survival and the probability of death. For short time intervals Δt and μ sufficiently smooth,

$${}_{\Delta t}p_x = e^{-\int_x^{x+\Delta t}\mu(s)\mathrm{d}s} \approx e^{-\frac{\Delta t}{2}\left(\mu(x)+\mu(x+\Delta t)\right)} \approx 1 - \Delta t \cdot \mu\left(x + \frac{\Delta t}{2}\right)$$

and

$${}_{\Delta t}q_x = 1 - e^{-\int_x^{x+\Delta t}\mu(s)\mathrm{d}s} \approx 1 - e^{-\frac{1}{2}\left(\mu(x)+\mu(x+\Delta t)\right)} \approx \Delta t \cdot \mu\left(x + \frac{\Delta t}{2}\right)$$

are useful approximations.

2.1 Parametric mortality models

For the parameter $\vartheta \coloneqq (\beta, \beta')$, the Gompertz model is the parametric model

$$\mu_\vartheta(x) = \beta' \cdot e^{\beta x},$$

while the Makeham model more generally is

$$\mu_\vartheta(x) = \alpha + \beta' \cdot e^{\beta x}; \tag{2.4}$$

here, the parameters are $\vartheta = (\alpha, \beta, \beta')$, where α is occasionally called the *Makeham term*. It combines a base mortality rate α with increasing mortality for increasing ages modelled by β and β'. The Siler model (Cohen et al. (2018)) adds two further parameters to better capture infant mortality and describes mortality as

$$\mu_\vartheta(x) = \alpha + \beta_i' \cdot e^{-\beta_i x} + \beta' \cdot e^{\beta x}. \tag{2.5}$$

[4]Note, that necessarily $\mu \geq 0$ and $M(x) = \int_0^x \mu(s)\mathrm{d}s \to \infty$ as $x \to \infty$.

Based on the Akaike or Bayes information criteria, our data does not give evidence for the Siler model and further, the investigations do not focus on infant mortality but in contrast to the mortality of the elder fraction of the population. For this reason we start out with model (2.4), which we reformulate as

$$\mu_\vartheta(x) = \alpha + \beta\, e^{\beta(x-M)}. \tag{2.6}$$

The law of mortality (2.6) comes with a useful interpretation. Indeed, the quantity M is a characteristic age of the model, similar to the mode of the distribution (cf. Proposition 2.1 below), while β models the growth rate of the force of mortality. The mortality rate does not fall below the remaining quantity α, the baseline mortality rate.

2.2 Mortality of cohorts

Cohen et al. (2018) and Osmond (1985) investigate the population's mortality over time. They conclude that β does not vary significantly over time, while the model age M does. We follow these results and model mortality depending on time by

$$\mu_\vartheta(x,t) = \big(\alpha + \beta\, e^{\beta(x-M)}\big) \cdot e^{-\lambda(t-2020)}; \tag{2.7}$$

over time, the mortality decays exponentially with rate parameter λ and t is the moment when observing the mortality μ. In (2.7) we have chosen the reference year 2020 (i.e., the reference date 2020, Jan. 1st) for convenience. The explicit antiderivative of the extended and time dependent model (2.7) is

$$M_\vartheta(x,t) = \big(\alpha\, x + e^{\beta(x-M)}\big) \cdot e^{-\lambda(t-2020)}.$$

In what follows we collect the parameters in the set

$$\Theta \coloneqq \big\{\vartheta = (\alpha,\beta,M,\lambda)\colon\, \alpha \geq 0, \beta \geq 0, M \geq 0 \text{ and } \lambda \geq 0\big\}. \tag{2.8}$$

With the parameters chosen, we shall also write μ_ϑ and ${}_uq_{\vartheta;x}$, e.g.

The model (2.7) has the following characteristic.

Proposition 2.1 (Mode)**.** *The mode of the distribution with time dependent hazard rate* (2.7) *is*

$$M - \frac{2\alpha}{\beta^2} + \frac{\lambda}{\beta}(t-2020) + \mathcal{O}(\alpha^2). \tag{2.9}$$

Proof. The density attains its maximum at x_m if $F''(x_m) = 0$ and the characterizing equation

$$\mu'(x_m) = \mu(x_m)^2$$

follows from (2.1). Based on the hazard rate (2.7) define the function

$$\begin{aligned} g(x;\alpha) &\coloneqq \mu_{\alpha,\beta,M,\lambda}(x)^2 - \mu'_{\alpha,\beta,M,\lambda}(x) \\ &= \big(\alpha + \beta\, e^{\beta(x-M)}\big)^2\, e^{-2\lambda(t-2020)} - \beta^2\, e^{\beta(x-M)-\lambda(t-2020)} \end{aligned} \tag{2.10}$$

and observe that

$$g\Big(M + \frac{\lambda}{\beta}(t-2020); 0\Big) = 0.$$

It follows that $x_m = M + \frac{\lambda}{\beta}(t-2020)$ is the mode of the Gompertz law.

The derivative of (2.10) with respect to x is

$$\frac{\partial}{\partial x} g(x;\alpha) = 2\big(\alpha + \beta\, e^{\beta(x-M)}\big) e^{-2\lambda(t-2020)}\, \beta^2 e^{\beta(x-M)} - \beta^3\, e^{\beta(x-M)-\lambda(t-2020)},$$

and with respect to α

$$\frac{\partial}{\partial \alpha} g(x;\alpha) = 2\big(\alpha + \beta\, e^{\beta(x-M)}\big) e^{-2\lambda(t-2020)}.$$

Evaluated at $x = M + \frac{\lambda}{\beta}(t-2020)$ and $\alpha = 0$, these quantities are

$$\frac{\partial}{\partial x} g\Big(M + \frac{\lambda}{\beta}(t-2020); 0\Big) = 2\beta^3 - \beta^3$$

and

$$\frac{\partial}{\partial \alpha} g\Big(M + \frac{\lambda}{\beta}(t-2020); 0\Big) = 2\beta.$$

By the implicit function theorem it follows that the solution $x_m(\alpha)$ of $g\big(x_m(\alpha);\alpha\big) = 0$ has derivative

$$\frac{d}{d\alpha} x_m(\alpha) = -\frac{\frac{\partial}{\partial \alpha} g}{\frac{\partial}{\partial x} g} = -\frac{2}{\beta^2}$$

and hence the assertion (2.9). □

Remark 2.2. The mode of the distribution (2.7) can be given even explicitly, but the formula is overly involved and does not reveal its main characteristics as (2.9) does.

Remark 2.3. We want to emphasize that the mortality improves at a rate λ according to the model (2.7), but the mode grows at the different rate $\frac{\lambda}{\beta}$. Further, the mode is *not* the average life expectancy and does not allow direct conclusions on the average life expectancy.

Remark 2.4 (Limitation of the model). We will give strong empirical evidence for the model (2.7) below and the result in Proposition 2.1 is in line with the report Rischatsch et al. (2018) for an observation period of about 100 years. However, the mode in (2.9) grows linearly with time t. Even at small growth rates $\frac{\lambda}{\beta}$, this is not overly realistic for observations periods covering multiple generations.

Remark 2.5. The mortality improvement in (2.7) depends on t, the calendar year of the observation. This is in line with actuarial practice for life insurance. For pension insurance contracts it is not the actual year t which matters for the life table, but the year of birth. The model (2.7) then modifies to

$$\mu_\vartheta(x,t) = \big(\alpha + \beta\, e^{\beta(x-M)}\big) \cdot e^{-\lambda(x+t-2020)}$$

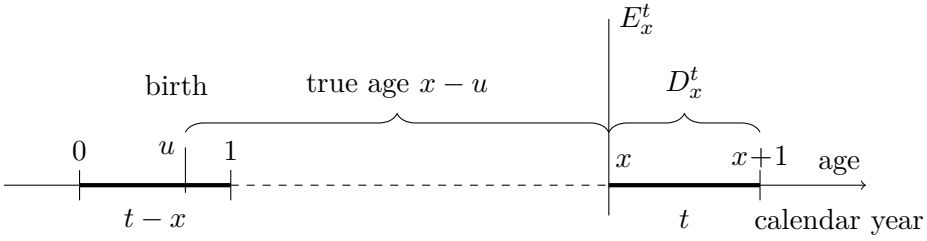

Figure 1: Calendar years and age

with antiderivative

$$M_\vartheta(x,t) = \left(-\frac{\alpha}{\lambda} + \frac{\beta}{\beta-\lambda}\, e^{\beta(x-M)}\right) \cdot e^{-\lambda(x+t-2020)}.$$

For the model to be meaningful from an actuarial perspective the additional constraint $\beta > \lambda$ is essential.

3 Estimation of parameters

In estimating longevity, a precise estimate of the parameters is of crucial importance. Various methods have been developed and investigated in the past to estimate the survival probabilities.

These include the classical method of Lee-Carter (see Lee and Carter (1992)) and ordinary least squares (OLS) approaches. Here we have to deal with several data issues as multiply censored data, particularly with varying and particularly differing groups of deaths and exposures. For this we employ the maximum likelihood method, which is known to be asymptotically unbiased and efficient. However, it is of importance to adapt the likelihood function to the censored data available. In what follows we outline the specific and essential modifications and our solution approach to adapt the method to the data available.

Recall that the ordinary likelihood of independent observations X_i is the product of its densities and hence, with (2.1),

$$L(\vartheta) = \prod_{i=1}^{n} {}_{X_i}p_{\vartheta;0} \cdot \mu_\vartheta(X_i), \tag{3.1}$$

where X_i is the age at the time of death of the individual i, enumerated by $i = 1, \ldots, n$.

3.1 True age versus arithmetic age

The models in Section 2 and the likelihood $L(\vartheta)$ in (3.1) involve the true age of an individual, represented by a (non-negative) real number. However, in the context of insurance the age x is typically simply today's calendar year minus the calendar year of birth, i.e., an integer (including 0) and so is the data available to us. Figure 1 illustrates

that the true age of an individual at age x is between $x-1$ and x if measured at the beginning of the current calendar year, but between x and $x+1$ at the end.

Full observations of the lives from birth to death at age X_i are usually not available neither. Typical observations of lives in insurance companies start at some age x_i, and they survive the period u_i, or they die within the observation period at age X_i. Let the subset $d \subset \{1,\dots,n\}$ collect the individuals with deaths observed throughout the observation period. The likelihood function of the censored data thus is

$$L(\vartheta) = \prod_{i\in d} \mu_\vartheta(X_i) \cdot {}_{X_i-x_i}p_{\vartheta;x_i} \cdot \prod_{i\in\{1,\dots,n\}\setminus d} {}_{u_i}p_{\vartheta;x_i},$$

Exact ages of the individual's death is typically not available neither; in contrast, it is only known that D_x many individuals out of E_x did not survive.

To model the integral ages discussed above (and illustrated in Figure 1) we follow common practice and assume that actual births and deaths occur uniformly distributed within the corresponding annual periods. The likelihood function thus modifies to

$$L(\vartheta) = \prod_x {}_uq_{\vartheta;x}^{D_x} \cdot \prod_x {}_up_{\vartheta;x}^{E_x-D_x},$$

where u is the observation period for each individual and the product ranges among all observed ages $x = 0, 1, 2, \dots$.

It follows that the average age of all exposures E_x is about $x - \frac{1}{2}$, while the average age of an individual dying in the current year is x. For this reason the likelihood function modifies as

$$L(\vartheta) = \prod_x {}_uq_{\vartheta;x}^{D_x} \cdot {}_up_{\vartheta;x-\frac{1}{2}}^{E_x-D_x},$$

if E_x are counted at the beginning of the year, cf. Figure 1. The corresponding log-likelihood is

$$\ell(\vartheta) = \sum_x D_x \ln\left({}_uq_{\vartheta;x}\right) + (E_x - D_x)\ln\left({}_up_{\vartheta;x-\frac{1}{2}}\right). \tag{3.2}$$

Remark 3.1 (Comparison with the binomial model). Assuming a random variable $X \sim \mathrm{bin}(q_x, E_x)$ with success probability q_x and population E_x, the likelihood involving all observations is

$$L(\vartheta) = \prod_{x=0} \binom{E_x}{D_x} q_x^{D_x}(1-q_x)^{E_x-D_x},$$

with corresponding log-likelihood

$$\ell(\vartheta) = \sum_{x=0} \ln\binom{E_x}{D_x} + D_x \ln q_x + (E_x - D_x)\ln(1-q_x).$$

As the binomial distribution itself is the composition of independent Bernoulli variables, the latter expression is notably of the same form as (3.2). Further, $\sum_{x=0} \ln\binom{E_x}{D_x}$ is a constant and hence does not impact the position of the parameter $\vartheta \in \Theta$ maximizing the likelihood. The maximum likelihood estimator for the independent observations and the binomial model thus coincide.

3.2 Aggregate ages

The data available to us are, in additional, aggregated, they are not accessible in the form (3.2). The data available accumulate deaths for different groups of ages as $g = \{85, 86, \dots, 89\}$, etc. To incorporate this missing information in the likelihood function consider

$$\ell(\vartheta) = \sum_x D_x \ln\left({}_uq_{\vartheta;x}\right) + (E_x - D_x) \ln\left({}_up_{\vartheta;x-\frac{1}{2}}\right), \tag{3.3}$$
$$\text{where } D_x \geq 0 \text{ and } \sum_{x\in g} D_x = D_g \text{ for all } g \in G.$$

Note, that D_x is not known in the formulation (3.3), but it is a constraint in the optimization procedure when computing the maximum likelihood. That is, the set of parameters is

$$\Theta = \left\{ \vartheta = (\alpha, \beta, M, \lambda, D_x^t) \;\middle|\; \begin{array}{l} \alpha \geq 0, \beta \geq 0, M \geq 0, \lambda \geq 0, \\ D_x^t \geq 0 \text{ for all } x \text{ and} \\ \sum_{x\in g} D_x^t = D_g^t \text{ for all groups } g \text{ and } t \end{array} \right\}.$$

This parametric set corresponds to augmenting the initial parameter space Θ in (2.8) by the $|g| - 1$-dimensional variable space containing D_x for all $x \in g$. The maximum likelihood estimator usually solves an unconstrained optimization problem, but aggregate data notably leads to a constraint optimization problem.

3.3 Generations

The model (2.7) employs the additional parameter t, which accounts for the different generations and their varying life tables with increasing life expectancy. The expositions E_x^t and deaths D_g^t count the individuals at ages in calendar year t. With this the likelihood (3.3) is

$$\ell(\vartheta) = \sum_{t=1990}^{2017} \sum_x D_x^t \ln\left({}_uq_{\vartheta;x}\right) + (E_x^t - D_x^t) \ln\left({}_up_{\vartheta;x-\frac{1}{2}}\right), \tag{3.4}$$
$$\text{with } D_x^t \geq 0 \text{ and } \sum_{x\in g} D_x^t = D_g^t \text{ for all } g \in G \text{ and } t, \tag{3.5}$$

with appropriate counts available in the years 1990 to 2017. As above, this likelihood incorporates the parameters D_x^t, which are only connected by the linking constraint $\sum_{x\in g} D_x^t = D_g^t$ for all $g \in G$ in (3.5).

3.4 Comprised problem formulations

The quantities p_ϑ and q_ϑ are given explicitly in (2.2) and (2.3). It follows that the general likelihood (3.4) is finally

$$\ell(\vartheta) = \sum_{t=1990}^{2017} \sum_{x=0}^{110} D_x^t \ln\left(1 - e^{-\left(M_\vartheta(x+1,t) - M_\vartheta(x,t)\right)}\right) \tag{3.6}$$
$$- \left(E_x^t - D_x^t\right)\left(M_\vartheta(x+\tfrac{1}{2},t) - M_\vartheta(x-\tfrac{1}{2},t)\right),$$
$$\text{with } D_x^t \geq 0 \text{ and } D_g^t = \sum_{x\in g} D_x^t \text{ for all } g \in G \text{ and } t.$$

Remark 3.2. For numerical stability in (3.6) we want to mention the approximation

$$1 - e^{-x} = \frac{x}{x + e^{-x/2}} + \mathcal{O}(x^3)$$

with high precision for small x, values in $(0,1)$, and precisely covering the tail for $x \gg 1$ ($x \to \infty$) equally well. This approximation is particularly useful during the learning phase of the approximation algorithm, as numerical algorithms often tend to test small and large values of x equally well.

4 Estimators and model evidence

4.1 The data

We have three sets of data available. We employ the first set from the Human Mortality Database (2021) for the period $t = 1990$ to $t = 2017$ as training data to compute the parameters, particularly the improvement rate λ of the force of mortality. This result is tested and used as a starting point to investigate the mortality with the particularly increased mortality rate at the end of the year 2020 and at the beginning of 2021.

The training data available includes the exposures E_x^t and observed deaths D_x^t for the period of $t = 1990$ to $t = 2017$, the ages $x = 0$ up to $x = 110$ and for both sexes, women and men. Observations of deaths, however, are accumulated in groups and for this reason it is essential to fall back to the parametric setting characterized by the set Θ in (3.6). German Federal Statistical Office: Statistisches Bundesamt (Destatis) (2021) reports weekly data of deaths from 2016 up to present, they are presented also in Table 1. Finally, to merge both data sets and the models we compute the expected deaths based on yearly population forecasts also provided from German Federal Statistical Office: population data in table S (2021) from 2016 to 2020 in order to compare actually observed deaths and the deaths expected by our model. The population at the beginning of 2021 is not available. For this reason we assume that the difference compared to 2020 is only marginal.

Figure 2 displays the mortality data available between $t = 1990$ and $t = 2017$ on a logarithmic scale for female and male and for different years of observation; the estimator employed here is

$$\hat{q}_x^t = D_x^t / E_x^t, \tag{4.1}$$

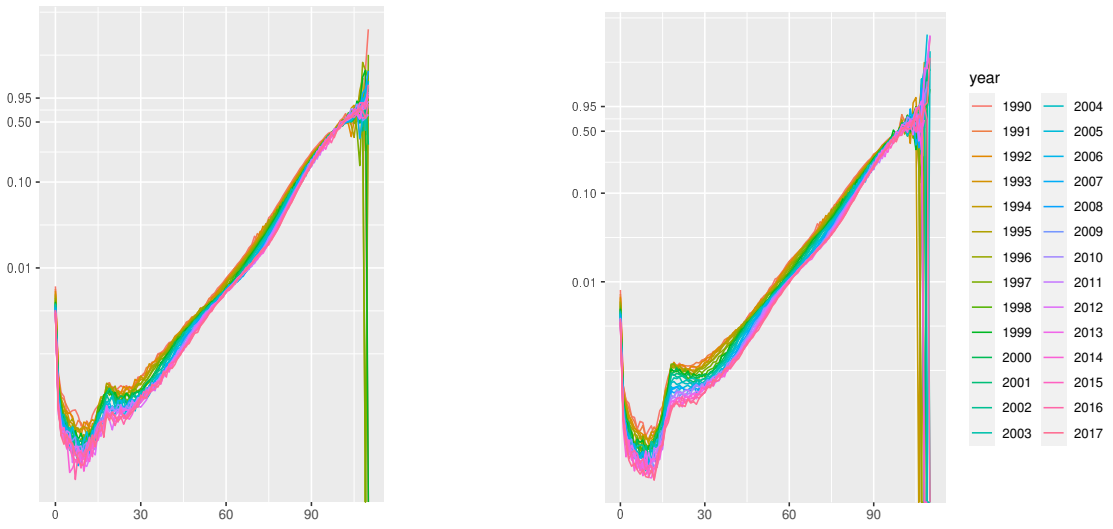

(a) female (b) male

Figure 2: Empirical mortality rates, Germany

deaths	Jan	Feb	Mar	Apr	May	Jun	Jul	Aug	Sep	Oct	Nov	Dec
2021	106.2	81.6	81.1	81.0								
2020	85.4	80.1	87.5	83.9	75.8	72.2	73.8	78.7	74.1	79.7	86.1	108.7
2016–2019	87.0	83.5	90.1	76.4	75.1	70.4	74.0	73.6	69.8	75.6	76.3	82.6

Table 1: Deaths observed per month; rounded to thousands

the empiric, non-smoothed mortality rate. The color scheme in the figure gives evidence that mortality is improving uniformly within the observation period of about 30 years between 1990 and 2017.

Remark 4.1. The estimators start to fluctuate heavily for ages of 90 years and older, apparently as the quantities E_x ($x \geq 90$) in this segment of the population get too small for the estimator (4.1) to be reliable.

observation	mode M in years	α	β	λ/ year
female	89.1	3.67 ‰	12.8 %	1.78 %
male	86.7	3.39 ‰	10.7 %	2.90 %

Table 2: Parameters describing the mortality of the German population

4.2 Parameters characterizing the mortality of the German population

We have tested the Siler model (2.5) versus the parametric model (2.6) by employing the Akaike and Bayes information criteria; both do not give evidence to model infant mortality in addition and for this it is justified to stick to the model (2.7), which involves mortality rates, which improve over time in addition.

Table 2 presents computational results for our data. The parameters give evidence that female live longer than men, as female's mode M exceed men's mode. The baseline probability α, in contrast, is somewhat lower for men then for women, but this quantity has only a minor influence to the overall mortality. It is interesting as well that mortality improves gradually over time with a rate of $\lambda = 1.78\,\%$ for women and $\lambda = 2.90\,\%$ for men, i.e., the probabilities improve faster for men. From the parameters in Table 2 it is clear, however, that mortality rates of men and women differ, and they have to be investigated separately.

In a long-term study including many countries of the Western world, Rischatsch et al. (2018, page 2) report that mortality improves by around $1\,\% - 2\,\%$ per year for both sexes. This is in line with our results for λ in Table 2, with the mortality of men in our sample improving faster. As well, we want to mention that, according to Rischatsch et al. (2018, Figure 1) again, the average life expectancy increased from about 40 years in 1860 to about 80 years in 2016 for countries of the Western world, which is an improvement of about $26\,\%$, i.e., 26 years in improved life expectancy per century for both sexes. Following (2.9) in Proposition 2.1, the mode improves at the rate $\frac{\lambda}{\beta}$, for which Table 2 reveals the quantities

$$\frac{\lambda}{\beta} \approx 14 \text{ years per century for women, and}$$
$$\frac{\lambda}{\beta} \approx 28 \text{ years per century for men.}$$

These external sources thus affirm our results.

Remark 4.2 (cf. Remark 2.3). We want to emphasize that the mode M in the model (2.7) and Table 2 is not the average expected life expectancy. Proposition 2.1 explains that the mode depends on all model parameters M, α, β and λ and outlines the relationship. Most importantly, the data are collected between 1990 and 2017, so that $2020 - t \approx 16.5$, on average. Hence, the mortality improvement rate must not be neglected.

Figure 3 displays the 1-year-mortalities $\hat{q}_{\vartheta;x}$ based on the parametric model (2.7) for varying observation years together with the rough estimates $\hat{q}_x$ from Figure 2. These displays, together with the literature referenced above, give evidence for the modelling approach chosen, i.e., to the model (2.7).

The displays in Figure 4 highlight elder ages. The rough estimator (4.1) and the smoothed version $\hat{q}_{\vartheta;x}$ coincide up to the age of 90, say, for women, and even up to the age of 100 for men. For extremely large ages, the rough estimators $\hat{q}_x$ are not reliable any longer due to the narrowing data, while $\hat{q}_{\vartheta;x}$ still can serve as reliable proxy. The chart

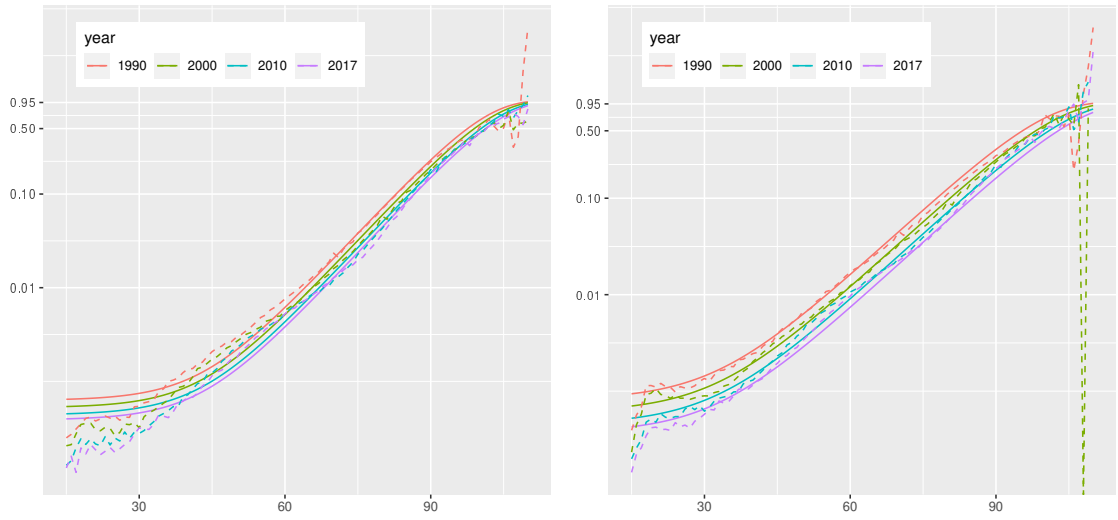

(a) female (b) male

Figure 3: One year probabilites $\hat{q}_x$ and the fitted model $\hat{q}_{\vartheta;x}$, derived from the data source

score	1990–2017	2020	2021
female	13.5 (−2.2)	19.9 (9.7)	22.1 (11.9)
male	13.7 (−0.6)	14.5 (9.9)	16.8 (13.0)

Table 3: Score (4.3), in brackets is the bias. The values in 2020 and 2021 are based on weekly data.

in Figure 4b for men exposes a larger bandwidth than Figure 4a, which is a consequence of the rate λ driving the decay of the mortality.

Figure 5 displays the mortality trend for specific ages (cf. Proposition 2.1). These mortality rates decrease linearly over time on the logistic scale. Further, the decay observed is uniform among all ages displayed. Again, this provides evidence in favor of the parameter λ in the model (2.7).

4.3 Model validation

The one-year probability of death is ${}_1q_x$ and, for this reason, the survival distribution of each individual follows a Bernoulli distribution. The collection of all individuals at age x is binomially distributed,[5]

$$D_x^t \sim \text{bin}({}_1q_x^t, E_x^t). \tag{4.2}$$

[5]Note, that ${}_1q_x$ in (4.2) is the *true* value.

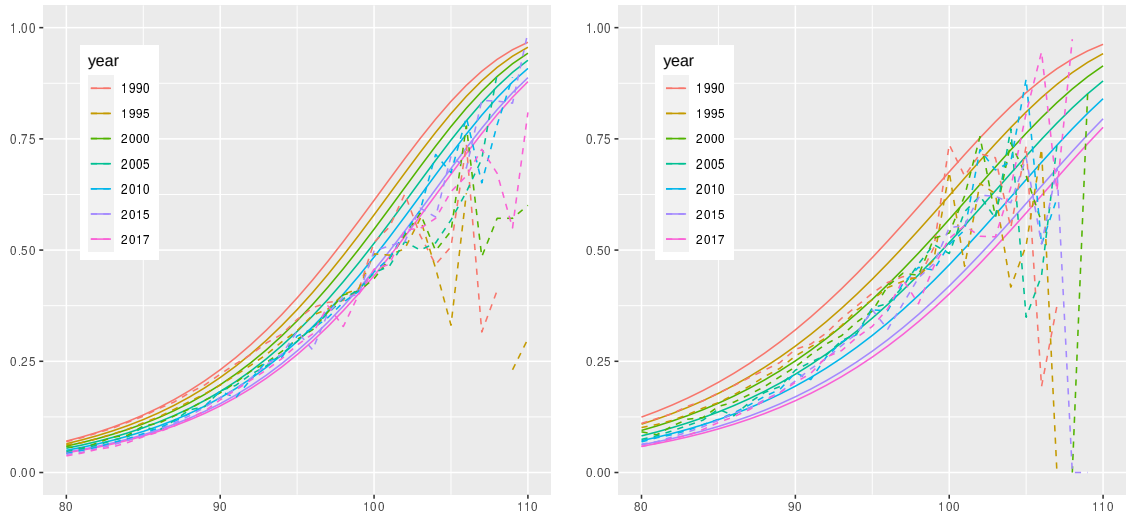

(a) female (b) male

Figure 4: Mortality rates of elderly people

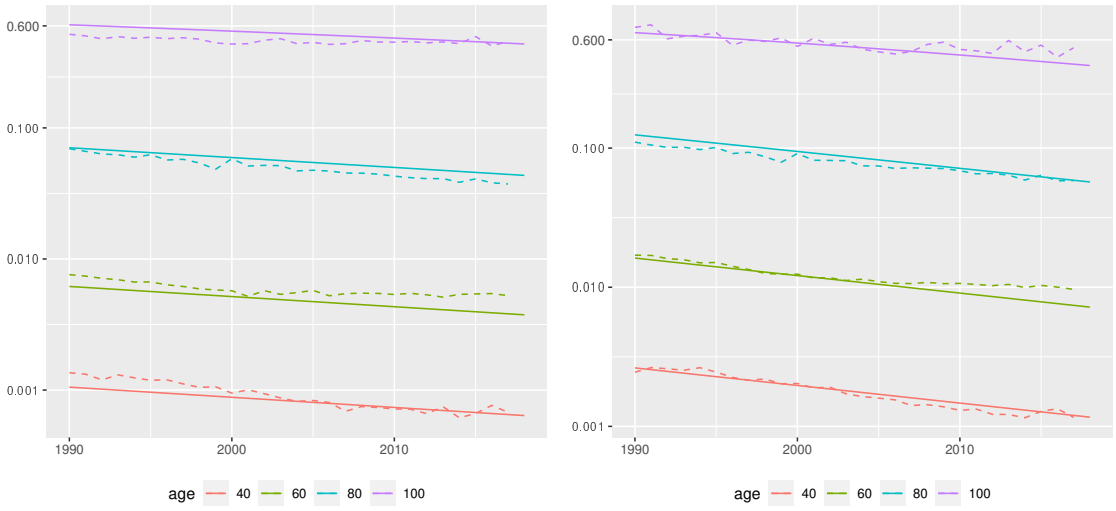

(a) female (b) male

Figure 5: Trend of selected mortality rates

This identity (4.2) indicates to study the derived standardized quantity

$$\frac{D_x^t - q_x\, E_x^t}{\sqrt{(1-q_x) q_x\, E_x^t}}, \tag{4.3}$$

i.e., the Z-score, or standard score. Note, that the score (4.3) $\gg 1$ indicates excess mortality. We shall refer to (4.3) simply as the *socre* and refer to Cairns et al. (2009, Equation (6.1)) for a similar quantity.

(i) For the estimator $\hat{q}_x = \frac{D_x^t}{E_x^t}$, the quantity (4.3) is 0;

(ii) for the true parameter q_x, (4.3) is normally distributed with standard parameters ($Z \sim \mathcal{N}(0,1)$);

(iii) for the parameter $q_{\vartheta;x}$, the score (4.3) is an important quantity of our further analysis, as positive aberrations indicate excess mortality. In what follows, the score is discussed and detailed further.

Figure 6 displays the distribution of the score (4.3) for the parameter $\hat{q}_{\vartheta;x}^t$ and exposes a standard deviation of about 14 for woman and men during the training period (see also Table 3). With that, the score in (4.3) can be rearranged to

$$q_{\vartheta;x} - \frac{D_x^t}{E_x^t} \;\approx\; \pm 14 \sqrt{\frac{(1-q_{\vartheta;x}) q_{\vartheta;x}}{E_x^t}}.$$

This exposes a quantitative comparison of the raw and the parametric estimator. Due to the term $\sqrt{q(1-q)}$ it is apparent as well that the estimators tend to deviate less with increasing exposures E_x^t and with the mortality parameter close to the boundary, i.e., with $\hat{q}_x \to 0$ and $\hat{q}_x \to 1$.

5 Historic mortality rates, compared to Covid-19: 2020 and 2021

The colors in Figure 6a are kind of symmetric around 0, even for elder individuals. Put differently, the score (4.3) does not indicate excess mortality during the training period up to 2017. Table 3 supports this evidence by exposing even negative biases during the training period 1990–2017, which is rather the contrary of excess mortality.

In contrast, Figure 6b exposes a different behavior and indicates high excess mortality, particularly of the population at age 85+. Table 3 amplifies this evidence by exposing higher scores and strict positive biases, in addition.

As well, these charts indicate that Covid-19 does not impact the mortality of younger population groups.

To elaborate the impact of mortality on Covid-19 further, Figure 7 compares quantities and scores from preceding sections with the year 2020 and the beginning of the

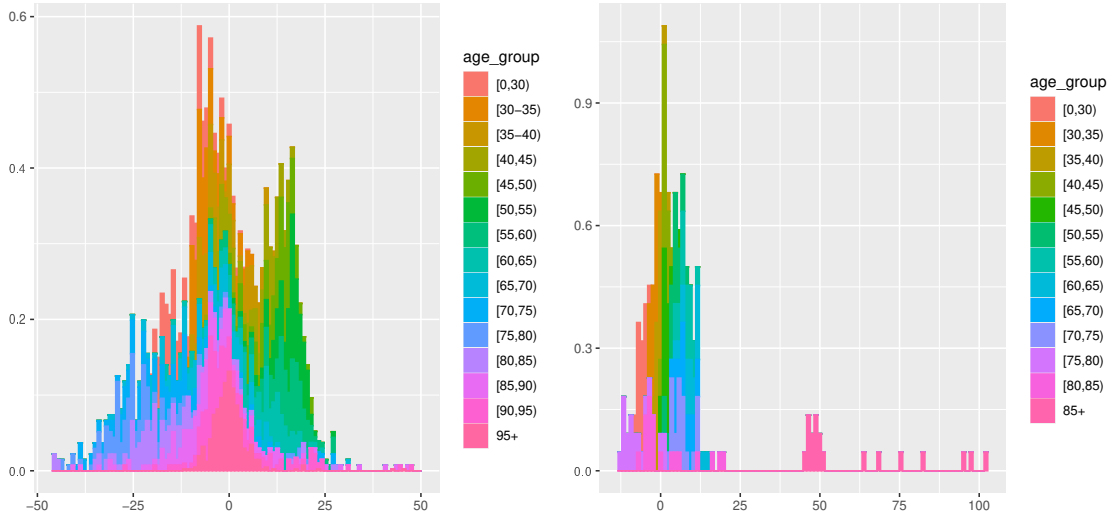

(a) (Annual) scores for all training data, 1990–2017

(b) Excess mortality: (weekly) score during the Covid-19 year 2021

Figure 6: Heatmap of the score (4.3) for varying ages: deviations to the right indicate excess mortality

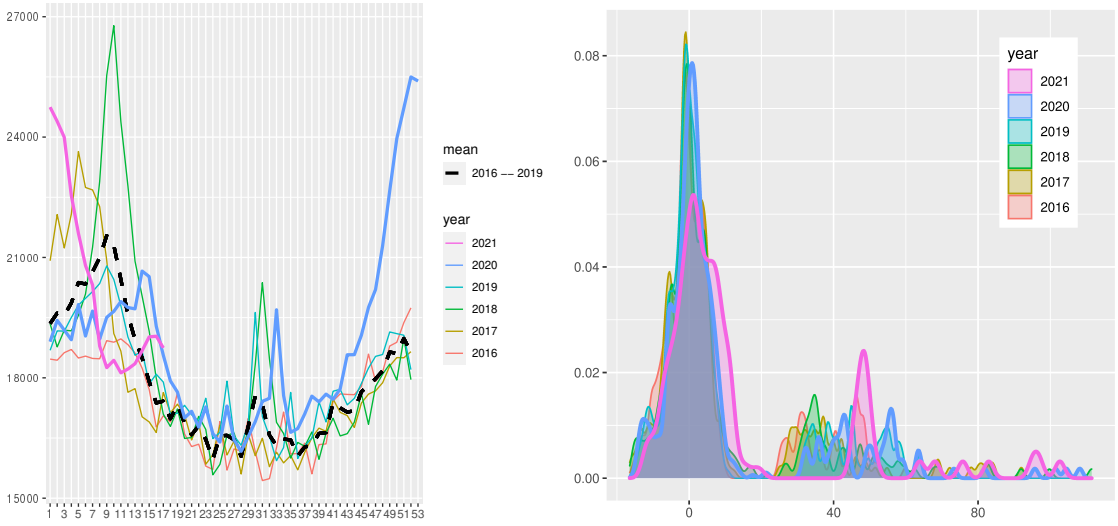

(a) Weekly observed deaths (total) during recent calendar years

(b) Density plot of the weekly scores (4.3) for different years: the displacement towards the right indicates excess mortality.

Figure 7: Is 2021 an outlier?

year 2021. Figure 7b compares the scores (4.3) for varying years instead of the varying ages displayed in Figure 6. As above, the plot is biased to the right particularly in the years 2021 and 2020, that is,

$$D_x \gg q_x E_x.$$

These are strong indicators for excess mortality. The Covid-19 years 2020 and 2021 exhibit additional peeks (with a score at 45 and 55, approximately).

Figure 7a (cf. also Table 1) displays the deaths observed in Germany with three striking peeks. The highest peek is at the end of the winter 2018, where a heavy flue epidemic caused excess mortality, with 27,000 deaths within a week, compared to 20,000 deaths in the same week of other years. The next important peek starting at the end of 2020 is caused by Covid-19; this peek continues in the first months of 2021. Here, the mortality exceeds 24,000 deaths per week, observed during several weeks, which is unprecedented in the last decades. It should be noted that this excess mortality was observed despite the fact that the country was in lockdown, or partial lockdown over several weeks. It is evident that the total mortality, without governmental countermeasures as the lockdown, would be significantly higher. Indeed, just recall that lethal traffic accidents or occupational accidents were much lower during that time, but still, the mortality was significantly higher than in comparable years without Covid-19. For completeness of the discussion, we emphasize that we only assess total mortality, i.e., we do not involve the medical cause of death. In particular, we do not distinguish in individuals died with Covid-19, because of Covid-19 or without Covid-19. We derive the conclusions from overall and total mortality only.

From a different perspective, the impacts of governmental countermeasures become evident as well by comparing the Figure 7a with deaths from Germany with other countries as the U.S., for example.

6 Discussion and summary

We employ an elementary parametric model to investigate German excess mortality during the Covid-19 pandemic in 2020 and the beginning of 2021. Base on the scarce data available during the pandemic we record, detect and measure excess morality of the elder population. It is evident that governmental countermeasures as strict lockdowns were successful. Otherwise, the mortality would have been significantly higher, as can be derived from the plots extracted from the data available.

From an actuarial perspective we provide evidence for excess mortality. Governmental countermeasures, however, are appropriate and adequate to limit the impacts significantly. Life and pension insurance companies (will) observe moderate excess mortality for elder people. There is not enough evidence for excess mortality for midlife ages, as the countermeasures by the state were adequate and appropriate to absorb the lethal impact.

References

N. Brouhns, M. Denuit, and J. K. Vermunt. A Poisson log-bilinear regression approach to the construction of projected lifetables. *Insurance: Mathematics and Economics*, 31(3):373–393, 2002. doi:10.1016/s0167-6687(02)00185-3. 3

A. J. G. Cairns. A discussion of parameter and model uncertainty in insurance. *Insurance: Mathematics and Economics*, 27(3):313–330, 2000. doi:10.1016/S0167-6687(00)00055-X. 2

A. J. G. Cairns, D. P. Blake, and K. Dowd. Modelling and management of mortality risk: A review. *Scandinavian Actuarial Journal*, 2-3:79–113, 2008. doi:10.2139/ssrn.1339970. 2

A. J. G. Cairns, D. Blake, K. Dowd, G. D. Coughlan, D. Epstein, A. Ong, and I. Balevich. A quantitative comparison of stochastic mortality models using data from England and Wales and the United States. *North American Actuarial Journal*, 13(1):1–35, 2009. doi:10.1080/10920277.2009.10597538. 3, 15

A. J. G. Cairns, D. P. Blake, A. Kessler, and M. Kessler. The impact of COVID-19 on future higher-age mortality. *SSRN Electronic Journal*, 2020. doi:10.2139/ssrn.3606988. 3

J. E. Cohen, C. Bohk, and R. Rau. Gompertz, Makeham, and Siler models explain Taylor's law in human mortality data. *Demographic Research*, 38:773–842, 2018. doi:10.4054/demres.2018.38.29. 3, 4, 5

I. D. Currie, M. Durban, and P. H. C. Eilers. Smoothing and forecasting mortality rates. *Statistical Modelling*, 4(4):279–298, 2004. doi:10.1191/1471082X04st080oa. 2

C. Czado, A. Delwarde, and M. Denuit. Bayesian Poisson log-bilinear mortality projections. *Insurance: Mathematics and Economics*, 36(3):260–284, 2005. doi:10.1016/j.insmatheco.2005.01.001. 2

L. A. Gavrilov and N. S. Gavrilova. Mortality measurement at advanced ages: A study of the social security administration death master file. *North American Actuarial Journal*, 12(3):432–447, 2011. doi:10.1080/10920277.2011.10597629. 3

H. U. Gerber. *Life Insurance Mathematics*. Springer-Verlag Berlin and Heidelberg, 3rd edition, 1997. doi:10.1007/978-3-662-03460-6. 3

German Federal Statistical Office: population data in table Statistisches Bundesamt (Destatis). Population data by gender, age and year in table 12411-0006:, 2021. URL `https://www-genesis.destatis.de/genesis/`. 10

German Federal Statistical Office: Statistisches Bundesamt (Destatis). https://www.destatis.de/DE/Themen/Gesellschaft-Umwelt/Bevoelkerung/Sterbefaelle- Lebenserwartung/sterbefallzahlen.html (data retrieved 2021-05-25)., 2021. 10

Human Mortality Database. University of California, Berkeley (USA), and Max Planck Institute for Demographic Research (Germany). Available at www.mortality.org or www.humanmortality.de (data retrieved on 2021-02-09)., 2021. URL `https://www.mortality.org/Public/UserAgreement.php`. 10

R. D. Lee and L. R. Carter. Modeling and forecasting U.S. mortality. *Journal of the American Statistical Association*, 87(419):659–671, 1992. doi:10.2307/2290201. 7

T. I. Missov, A. Lenart, L. Nemeth, V. Canudas-Romo, and J. W. Vaupel. The Gompertz force of mortality in terms of the modal age at death. *Demographic Research*, 32:1031–1048, 2015. doi:10.4054/demres.2015.32.36. 2

L. Németh, D. A. Jdanov, and V. M. Shkolnikov. An open-sourced, web-based application to analyze weekly excess mortality based on the short-term mortality fluctuations data series. *PLOS ONE*, 16(2):e0246663, 2021. doi:10.1371/journal.pone.0246663. 3

C. Osmond. Using age, period and cohort models to estimate future mortality rates. *International Journal of Epidemiology*, 14(1):124–129, 1985. doi:10.1093/ije/14.1.124. 2, 5

A. Pichler. Construction of life tables. *Blätter der Deutschen Gesellschaft für Versicherungsmathematik*, 23:107–119, 1997. doi:10.1007/BF02808245. 3

M. Rischatsch, D. Pain, D. Ryan, and Y. Chiu. Mortality improvement: understanding the past and framing the future. *Swiss Re, sigma*, 6, 2018. 6, 12

C. Wong-Fupuy and S. Haberman. Projecting mortality trends. *North American Actuarial Journal*, 8(2):56–83, 2004. doi:10.1080/10920277.2004.10596137. 2